Available online at www.sciencedirect.com
SCIENCE DIRECT®
ELSEVIER
International Journal of Solids and Structures 43 (2006) 1960–1978
INTERNATIONAL JOURNAL OF SOLIDS and STRUCTURES
www.elsevier.com/locate/ijsolstr

Effect of built-in edges on 3-D vibrational characteristics of thick circular plates

D. Zhou [a,*], F.T.K. Au [b], Y.K. Cheung [b], S.H. Lo [b]

[a] *Department of Mechanics and Engineering Science, Nanjing University of Science and Technology, Nanjing 210014, People's Republic of China*
[b] *Department of Civil Engineering, The University of Hong Kong, Pokfulam Road, Hong Kong*

Received 7 December 2004; received in revised form 5 May 2005
Available online 1 July 2005

Abstract

The vibrational characteristics of thick circular plates built into a rigid medium in the vicinity of the circumference are studied. The analysis procedure is based on the exact, small-strain, three-dimensional linear elasticity theory. In the analysis, the plate is considered as comprising an inner circular disc with free upper and lower surfaces connected to an outer annulus that is built into the rigid medium. The Chebyshev polynomials multiplied by suitable boundary characteristic functions are selected as the admissible functions of the displacement functions, and the three-dimensional displacement fields in each part can be expressed accordingly. Through the Ritz method, the eigenvalue equations can be established for the inner disc and the outer annulus, respectively. Utilizing the displacement continuity conditions at the interface between the two parts, the eigenvalue equation for the whole plate is derived. Convergence and comparison studies demonstrate the correctness and accuracy of the present method. The effect of structural parameters such as plate thickness, built-in length and the end condition on eigenfrequencies of circular plate is investigated in detail. It is shown that with the increase of plate thickness, the effect of the built-in annulus on eigenfrequencies significantly increases. Therefore, for a thick plate, the flexibility of the built-in part should be considered in the dynamic analysis.

Keywords: Built-in edge; Eigenfrequency; Free vibration; Thick circular plate; Three-dimensional analysis

* Corresponding author. Tel.: +86 25 84316695; fax: +86 2585416677.
E-mail address: dingzhou57@yahoo.com (D. Zhou).

0020-7683/$ - see front matter © 2005 Elsevier Ltd. All rights reserved.
doi:10.1016/j.ijsolstr.2005.05.007

1. Introduction

In view of the wide applications of circular plates in many practical fields such as civil, defence, marine and mechanical engineering, numerous investigations in this area have been carried out over the years. A summary of the early research achievements on vibration of circular plates was given by Leissa (1969). So and Leissa (1998) pointed out that up to now, at least 90% of the published results are based upon two-dimensional (2-D) plate theories. It is well known that the classical plate theory (CPT) can provide accurate results for sufficiently thin plates, but it always overestimates eigenfrequencies due to the Kirchhoff hypothesis. To improve the accuracy of the CPT and extend it to moderately thick plates, Deresiewicz and Mindlin (1955) presented the first-order shear deformation theory (FSDT) by including shear and rotary inertia. Liew et al. (1997) used the differential quadrature method to study the free vibration of circular Mindlin plates. Moreover, various higher-order shear deformation theories (HSDT) have also been developed (Reddy, 1984; Hanna and Leissa, 1994) for thick plates.

2-D plate theories reduce the dimension of problem from three to two by imposing certain assumptions on the deformations in the plate-thickness direction. This results in a relatively simple expression and derivation of solutions. These artificial constraints inherently bring errors, which rapidly increase with the plate thickness. Moreover, these simplified theories cannot predict a full free vibration spectrum for very thick plates. As a result, three-dimensional (3-D) elasticity theories play an important role not only in providing realistic results but also in bringing out physical insights, which cannot be obtained from 2-D theories.

In the recent two decades, some attempts on 3-D vibration analysis of circular plates have been reported. Hutchinson provided a Mathieu series solution for thick, circular plates with free edges (Hutchinson, 1979) and evaluated the validity of the FSDT (Hutchinson, 1984). So and Leissa (1998) used simple algebraic polynomials as admissible functions to calculate the eigenfrequencies of thick, completely free circular and annular plates using the Ritz method, while Liew and Yang (1999, 2000) used orthogonally generated polynomials as admissible functions to analyze such plates with various boundary conditions. Fan and Ye (1990) used the state-space method to investigate the free vibration of laminated circular plates, and Liu and Lee (2000) used the finite element method to analyze the vibration modes of circular plates. In two recent papers (Zhou et al., 2003a,b), the writers adopted Chebyshev polynomial series (Fox and Parker, 1968) as the admissible functions to study the 3-D vibration of circular and annular plates, and solid and hollow circular cylinders, respectively. The advantage of Chebyshev polynomials in numerical stability, in particular in the calculation of the higher-order modes has been shown.

In the existing 2-D and 3-D analyses of plates, classical boundary conditions are commonly used to represent the boundary constraints of the plate, such as clamped, free, simply-supported, sliding edges, etc. Note that for 3-D analysis, the simply-supported condition can be further divided into the hard and the soft cases. However, it should be pointed out that except for the completely free edge, other types of edge conditions such as the clamped or simply-supported ones cannot be exactly replicated in reality, as they are only approximate descriptions of the actual edge conditions (So and Leissa, 1998). Although such approximations are sufficiently accurate for thin plates, they may not be suitable for thick plates. Normally, if a plate is built into a rigid medium, then it is considered as a plate with clamped edges along the termination of the free upper and lower surfaces. Such a boundary description accords with the mechanical behavior of thin plates fairly well. However it would result in significant errors for thick plate analysis, because of the flexibility of the built-in part of the plate, which increases with increasing plate thickness. In actual practice, as a rule, the flexibility of the built-in part can be approximately considered as equivalent massless translational and/or torsional springs distributed along the edge of the inner disc or an equivalent size added to the radius of the inner disc. However, it is very difficult to correctly determine the equivalent stiffness or the equivalent size of the built-in part. In the present analysis, the effect of the size of built-in support and the plate thickness on vibrational characteristics of circular plates is studied in detail based on the 3-D linear elasticity theory. The Ritz method is used to derive the eigenvalue equation of the plate. The effect of the

flexibility of the built-in annulus on eigenfrequencies is investigated in detail. Some results known for the first time and some important conclusions are given.

2. Theoretical formulation

Consider a homogeneous and isotropic, annular plate with outer radius R_2 inner radius R_0 and thickness h, as shown in Fig. 1. It is clear that $R_0 = 0$ yields a solid circular plate. The outer annulus of the plate is built into a rigid medium while the inner annulus of the plate has free upper and lower surfaces. In addition, the outer edge of the plate may either be free or set in the rigid medium, as shown in Fig. 1(b). The latter case is hereafter called the fully built-in condition. The radius of the interface between the outer and inner annuluses (the interface radius) is R_1. Therefore, the radial built-in length of the plate is $R_2 - R_1$. A cylindrical coordinate system with r in the radial direction, θ in the circumferential direction and z in the thickness direction is developed to describe the motion of the plate. The corresponding displacement components at a generic point are u, v and w in the r, θ and z directions, respectively. Dividing the plate into two concentric annular plates (denoted by $i = 1,2$, respectively) will result in one with free upper and lower surfaces ($i = 1$) and another built into the rigid medium ($i = 2$). The displacements at surfaces in contact with the rigid medium are fully restrained but no initial clamping force on the built-in section in the thickness direction is assumed.

For each sub-plate, the linear elastic strain energy V^i is given by

$$V^i = \frac{G}{2}\int_{R_{i-1}}^{R_i}\int_0^{2\pi}\int_{-h/2}^{h/2}\left\{\frac{2v}{1-2v}\left(\varepsilon_{rr}^i+\varepsilon_{\theta\theta}^i+\varepsilon_{zz}^i\right)^2 +2\left[\left(\varepsilon_{rr}^i\right)^2+\left(\varepsilon_{\theta\theta}^i\right)^2+\left(\varepsilon_{zz}^i\right)^2\right]+\left(\varepsilon_{r\theta}^i\right)^2+\left(\varepsilon_{rz}^i\right)^2+\left(\varepsilon_{\theta z}^i\right)^2\right\} r\,\mathrm{d}z\,\mathrm{d}\theta\,\mathrm{d}r, \tag{1}$$

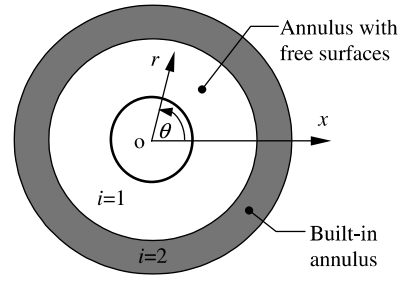

(a) Plan of plate

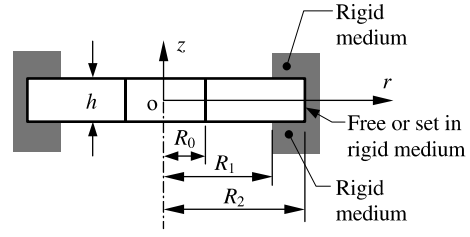

(b) Cross section through centre

Fig. 1. An annular plate built into a rigid medium.

where G is the shear modulus, v is the Poisson's ratio. ε^i_{st} $(s,t=r,\theta,z)$ are the strain components of the ith sub-plate as follows

$$\begin{aligned}&\varepsilon^i_{rr}=\frac{\partial u_i}{\partial r};\quad \varepsilon^i_{\theta\theta}=\frac{u_i}{r}+\frac{\partial v_i}{r\partial\theta};\quad \varepsilon^i_{zz}=\frac{\partial w_i}{\partial z},\\&\varepsilon^i_{r\theta}=\frac{\partial u_i}{r\partial\theta}+\frac{\partial v_i}{\partial r}-\frac{v_i}{r};\quad \varepsilon^i_{rz}=\frac{\partial u_i}{\partial z}+\frac{\partial w_i}{\partial r};\quad \varepsilon^i_{\theta z}=\frac{\partial v_i}{\partial z}+\frac{\partial w_i}{r\partial\theta}\end{aligned}\tag{2}$$

in which, u_i, v_i and w_i are the corresponding displacement components of the ith sub-plate in the r, θ and z directions, respectively.

The kinetic energy T^i of the ith sub-plate is given by

$$T^i=\frac{\rho}{2}\int_{R_{i-1}}^{R_i}\int_0^{2\pi}\int_{-h/2}^{h/2}\left[\left(\frac{\partial u_i}{\partial t}\right)^2+\left(\frac{\partial v_i}{\partial t}\right)^2+\left(\frac{\partial w_i}{\partial t}\right)^2\right]r\,\mathrm{d}z\,\mathrm{d}\theta\,\mathrm{d}r,\tag{3}$$

where ρ is the mass density per unit volume.

For simplicity in mathematical expression, the following dimensionless parameters are introduced

$$\bar r_i=\frac{2r}{\overline{R}_i}-\delta_i;\quad \bar\theta=\theta;\quad \bar z=\frac{2z}{h},\tag{4}$$

where $\overline{R}_i=R_i-R_{i-1}$ and $\delta_i=(R_i+R_{i-1})/(R_i-R_{i-1})$.

For free vibration, the displacement components of the plate can be written in terms of the displacement amplitude functions as follows

$$\begin{aligned}&u_i(r,\theta,z,t)=U_i(\bar r_i,\bar\theta,\bar z)\mathrm{e}^{\mathrm{j}\omega t};\quad v_i(r,\theta,z,t)=V_i(\bar r_i,\bar\theta,\bar z)\mathrm{e}^{\mathrm{j}\omega t};\\&w_i(r,\theta,z,t)=W_i(\bar r_i,\bar\theta,\bar z)\mathrm{e}^{\mathrm{j}\omega t},\end{aligned}\tag{5}$$

where ω denotes the eigenfrequency of the plate and $\mathrm{j}=\sqrt{-1}$.

Considering the circumferential symmetry of the circular plate about the coordinate $\bar\theta$, the displacement amplitude functions can be further expressed by

$$\begin{aligned}&U_i(\bar r_i,\bar\theta,\bar z)=\overline{U}_i(\bar r_i,\bar z)\cos(n\bar\theta);\quad V_i(\bar r_i,\bar\theta,\bar z)=\overline{V}_i(\bar r_i,\bar z)\sin(n\bar\theta);\\&W_i(\bar r_i,\bar\theta,\bar z)=\overline{W}_i(\bar r_i,\bar z)\cos(n\bar\theta),\end{aligned}\tag{6}$$

where n is the circumferential wave number, which should be taken to be an integer, namely $n=0,1,2,\ldots,\infty$, to ensure the periodicity of a circular plate. It is obvious that $n=0$ means the axisymmetric mode. In such a case, $U_i(\bar r_i,\bar\theta,\bar z)=\overline{U}_i(\bar r_i,\bar z)$; $V_i(\bar r_i,\bar\theta,\bar z)=0$; $W_i(\bar r_i,\bar\theta,\bar z)=\overline{W}_i(\bar r_i,\bar z)$. Rotating the symmetry axes by $\pi/2$, another set of free vibration modes can be obtained, corresponding to an interchange of $\cos(n\theta)$ and $\sin(n\theta)$ in Eq. (6). However, in such a case, $n=0$ means $U_i(\bar r_i,\bar\theta,\bar z)=0$; $V_i(\bar r_i,\bar\theta,\bar z)=\overline{V}(\bar r_i,\bar z)$ and $W_i(\bar r_i,\bar\theta,\bar z)=0$, which is referred to as the torsional mode.

In free vibration problems, the displacements of the plate are periodic functions of time and so are the corresponding potential energy and kinetic energy. Therefore, substituting Eqs. (4)–(6) into Eqs. (1)–(3) yields the maximum potential energy $V^i_{\max}$ and kinetic energy $T^i_{\max}$ of the ith sub-plate during a vibration cycle as follows

$$\begin{aligned}V^i_{\max}=&\frac{Gh}{2}\int_{-1}^{1}\int_{-1}^{1}\left\{\frac{2v}{1-2v}\Gamma_1(\bar\varepsilon^i_{\bar r\bar r}+\bar\varepsilon^i_{\bar\theta\bar\theta}+\bar\varepsilon_{\bar z\bar z^i})\right.\\&+2\Gamma_1[(\bar\varepsilon^i_{\bar r\bar r})^2+(\bar\varepsilon^i_{\bar\theta\bar\theta})^2+(\bar\varepsilon^i_{\bar z\bar z})^2]\\&\left.+\Gamma_2[(\bar\varepsilon^i_{\bar r\bar\theta})^2+(\bar\varepsilon^i_{\bar r\bar z})^2+(\bar\varepsilon^i_{\bar\theta\bar z})^2]\right\}(\bar r_i+\delta_i)\,\mathrm{d}\bar z\,\mathrm{d}\bar r_i;\\T^i_{\max}=&\frac{\rho\overline{R}_i^2h}{16}\omega^2\int_{-1}^{1}\int_{-1}^{1}\left(\Gamma_1\overline{U}_i^2+\Gamma_2\overline{V}_i^2+\Gamma_1\overline{W}_i^2\right)(\bar r_i+\delta_i)\,\mathrm{d}\bar z\,\mathrm{d}\bar r_i,\end{aligned}\tag{7}$$

$$\bar{\varepsilon}^i_{\bar{r}\bar{r}} = \frac{\partial \overline{U}_i}{\partial \bar{r}_i}; \quad \bar{\varepsilon}^i_{\bar{\theta}\bar{\theta}} = \frac{\overline{U}_i}{\bar{r}_i + \delta_i} + n\frac{\overline{V}_i}{\bar{r}_i + \delta_i}; \quad \bar{\varepsilon}^i_{\bar{z}\bar{z}} = \frac{\partial \overline{W}_i}{\gamma_i \partial \bar{z}},$$

$$\bar{\varepsilon}^i_{\bar{r}\bar{\theta}} = -\frac{n\overline{U}_i}{\bar{r}_i + \delta_i} + \frac{\partial \overline{V}_i}{\partial \bar{r}_i} - \frac{\overline{V}_i}{\bar{r}_i + \delta_i}; \quad \bar{\varepsilon}^i_{\bar{r}\bar{z}} = \frac{\partial \overline{U}_i}{\gamma_i \partial \bar{z}} + \frac{\partial \overline{W}_i}{\partial \bar{r}_i}; \tag{8}$$

$$\bar{\varepsilon}^i_{\bar{\theta}\bar{z}} = \frac{\partial \overline{V}_i}{\gamma_i \partial \bar{z}} - \frac{n\overline{W}_i}{\bar{r}_i + \delta_i}$$

in which,

$$\begin{aligned} \Gamma_1 &= \int_0^{2\pi} \cos^2(n\theta)\,\mathrm{d}\theta = \begin{cases} 2\pi & \text{if } n = 0, \\ \pi & \text{if } n > 0, \end{cases} \\ \Gamma_2 &= \int_0^{2\pi} \sin^2(n\theta)\,\mathrm{d}\theta = \begin{cases} 0 & \text{if } n = 0, \\ \pi & \text{if } n > 0, \end{cases} \quad \gamma_i = h/\overline{R}_i. \end{aligned} \tag{9}$$

Each of the displacement amplitude functions $\overline{U}_i(\bar{r}_i, \bar{z})$, $\overline{V}_i(\bar{r}_i, \bar{z})$ and $\overline{W}_i(\bar{r}_i, \bar{z})$ is assumed, respectively, in the form of double series of Chebyshev polynomials multiplied by boundary characteristic functions as follows

$$\begin{aligned} \overline{U}_i(\bar{r}_i, \bar{z}) &= \Phi^i_u(\bar{r}_i)\Psi^i_u(\bar{z}) \sum_{j=1}^{J_i} \sum_{k=1}^{K_i} A^i_{jk} F_j(\bar{r}_i) F_k(\bar{z}); \\ \overline{V}_i(\bar{r}_i, \bar{z}) &= \Phi^i_v(\bar{r}_i)\Psi^i_v(\bar{z}) \sum_{l=1}^{L_i} \sum_{m=1}^{M_i} B^i_{lm} F_l(\bar{r}_i) F_m(\bar{z}); \\ \overline{W}_i(\bar{r}_i, \bar{z}) &= \Phi^i_w(\bar{r}_i)\Psi^i_w(\bar{z}) \sum_{p=1}^{P_i} \sum_{q=1}^{Q_i} C^i_{mn} F_p(\bar{r}_i) F_q(\bar{z}), \end{aligned} \tag{10}$$

where J_i, K_i, L_i, M_i, P_i and Q_i are the truncated orders of the Chebyshev series and A^i_{jk}, B^i_{lm} and C^i_{pq} are the unknown coefficients. $F_s(\chi)$ $(s = 1, 2, 3, \ldots;\ \chi = \bar{r}_i, \bar{z}_i)$ is the one-dimensional sth Chebyshev polynomial which can be expressed in a form of cosine functions as follows

$$F_s(\chi) = \cos[(s-1)\arccos(\chi)]; \quad (s = 1, 2, 3, \ldots) \tag{11}$$

while $\Phi^i_u(\bar{r}_i)$, $\Phi^i_v(\bar{r}_i)$, $\Phi^i_w(\bar{r}_i)$, $\Psi^i_u(\bar{z})$, $\Psi^i_v(\bar{z})$ and $\Psi^i_w(\bar{z})$ are boundary characteristic functions of the ith sub-plate, which enable the displacement components u_i, v_i and w_i to satisfy the geometric boundary conditions of the sub-plate. It is obvious that $\Psi^1_u(\bar{z}) = \Psi^1_v(\bar{z}) = \Psi^1_w(\bar{z}) = 1$ because the upper and lower surfaces of the inner disc are free. For a solid circular plate, $\Phi^1_u(\bar{r}_1) = \Phi^1_v(\bar{r}_1) = \Phi^1_w(\bar{r}_1) = 1$. For a plate with fully built-in condition at the edge,

$$\Phi^2_u(\bar{r}_2) = \Phi^2_v(\bar{r}_2) = \Phi^2_w(\bar{r}_2) = 1 - \bar{r}_2; \quad \Psi^2_u(\bar{z}) = \Psi^2_v(\bar{z}) = \Psi^2_w(\bar{z}) = 1 - \bar{z}^2 \tag{12}$$

while for a plate with a built-in outer annulus but a free edge at $r = R_2$,

$$\Phi^2_u(\bar{r}_2) = \Phi^2_v(\bar{r}_2) = \Phi^2_w(\bar{r}_2) = 1; \quad \Psi^2_u(\bar{z}) = \Psi^2_v(\bar{z}) = \Psi^2_w(\bar{z}) = 1 - \bar{z}^2. \tag{13}$$

It is noted that Chebyshev polynomial series $F_s(\chi)$ $(s = 1, 2, 3, \ldots)$ is a set of complete and orthogonal one in the interval $[-1, 1]$. This ensures the double series $F_j(\chi)F_k(\chi)$ $(j, k = 1, 2, 3, \ldots)$ to be also a complete and orthogonal set in each sub-plate region. The excellent properties of the Chebyshev polynomial series in the approximation of functions have been well known (Fox and Parker, 1968). Therefore, using this set of Chebyshev polynomial series as the admissible functions, rapid convergence and excellent stability in numerical operation can be expected. However, in the Ritz method, the admissible functions should satisfy the specified geometric boundary conditions. Therefore, except for the completely free circular plates, the

boundary characteristic functions should be introduced to ensure the satisfaction of geometric boundary conditions, as given in Eq. (10). The boundary characteristic functions should be continuous and differentiable. Their sign should not change in the structural domain and they should also satisfy the geometric boundary conditions. Therefore the shapes of displacement amplitude functions are controlled by the Chebyshev polynomials, which are the main components of displacement amplitude functions.

For a structure with symmetric boundary conditions, the boundary characteristic functions should also be symmetric. The vibration modes can be classified into symmetric and antisymmetric ones by taking the even and odd terms of Chebyshev polynomial series, respectively. This will greatly reduce the computational effort.

Defining the energy functional of the ith sub-plate as

$$\Pi_i = V^i_{\max} - T^i_{\max} \tag{14}$$

and minimizing the above functional with respect to the coefficients as follows

$$\frac{\partial \Pi_i}{\partial A^i_{jk}} = 0; \quad \frac{\partial \Pi_i}{\partial B^i_{lm}} = 0; \quad \frac{\partial \Pi_i}{\partial C^i_{pq}} = 0 \tag{15}$$

one obtains the eigenvalue equations in matrix form of

$$([K^i] - \Omega^2[M^i])\{X^i\} = 0; \quad i = 1, 2, \tag{16}$$

where

$$\begin{aligned}
&\Omega = \omega R_1\sqrt{\rho/G}; \quad [K^i] = \begin{pmatrix} [K^{uui}] & [K^{uvi}] & [K^{uwi}] \\ & K^{vvi} & [K^{vwi}] \\ \text{Sym} & & [K^{wwi}] \end{pmatrix}; \\
&[M^i] = \left(\frac{R_i}{R_1}\right)^2 \begin{pmatrix} [M^{uui}] & [0] & [0] \\ & [M^{vvi}] & [0] \\ \text{Sym} & & [M^{wwi}] \end{pmatrix}; \\
&\{X^i\} = \{\{A^i\} \quad \{B^i\} \quad \{C^i\}\}^{\mathrm{T}}, \quad \text{for } n \geqslant 1,
\end{aligned} \tag{17}$$

$$\begin{aligned}
&[K^i] = \begin{pmatrix} [K^{uui}] & [K^{uwi}] \\ \text{Sym} & [K^{wwi}] \end{pmatrix}; \; [M^i] = \left(\frac{R_i}{R_1}\right)^2 \begin{pmatrix} [M^{uui}] & [0] \\ \text{Sym} & [M^{wwi}] \end{pmatrix}; \\
&\{X^i\} = \{\{A^i\} \quad \{C^i\}\}^{\mathrm{T}}, \quad n = 0 \quad \text{for the axisymmetric vibration}
\end{aligned} \tag{18}$$

$$[K^i] = [K^{vvi}]; \quad [M^i] = (\overline{R}_i/R_1)^2[M^{vvi}];$$

$$\{X^i\} = \{B^i\}^{\mathrm{T}}, \quad n = 0 \quad \text{for the torsional vibration.} \tag{19}$$

In the above equations, $[K^{sti}]$ and $[M^{sti}]$ $(s, t = u, v, w)$ are the stiffness sub-matrices and the diagonal mass sub-matrices of the ith sub-plate, respectively. $\{A^i\}$, $\{B^i\}$ and $\{C^i\}$ are column vectors composed of the unknown coefficients as follows

$$\begin{aligned}
\{A^i\} &= \{A^i_{11} \quad \cdots \quad A^i_{1K_i} \quad A^i_{21} \quad \cdots \quad A^i_{2K_i} \quad \cdots \quad A^i_{J_i1} \quad \cdots \quad A^i_{J_iK_i}\}^{\mathrm{T}}; \\
\{B^i\} &= \{B^i_{11} \quad \cdots \quad B^i_{1M_i} \quad B^i_{21} \quad \cdots \quad B^i_{2M_i} \quad \cdots \quad B^i_{L_i1} \quad \cdots \quad B^i_{L_iM_i}\}^{\mathrm{T}}; \\
\{C^i\} &= \left\{C^i_{11} \quad \cdots \quad C^i_{1Q_i} \quad C^i_{21} \quad \cdots \quad C^i_{2Q_i} \quad \cdots \quad C^i_{P_i1} \quad \cdots \quad C^i_{P_iQ_i}\right\}^{\mathrm{T}}.
\end{aligned} \tag{20}$$

The elements of the sub-matrices $[K^{sti}]$ and $[M^{sti}]$ $(s,t=u,v,w)$ are given by

$$
\begin{aligned}
[K^{uui}] &= \frac{1-v}{1-2v}\left(D^{i111}_{ujv\bar{j}} + D^{i00-1}_{uju\bar{j}}\right)H^{00}_{uku\bar{k}} + \frac{v}{1-2v}\left(D^{i010}_{uju\bar{j}} + D^{i100}_{uju\bar{j}}\right)H^{00}_{uku\bar{k}} \\
&\quad + \frac{1}{2\gamma_i^2}\left(n^2\gamma_i^2 D^{i00-1}_{uju\bar{j}}H^{00}_{uku\bar{k}} + D^{i001}_{uju\bar{j}}H^{11}_{uku\bar{k}}\right); \\
[K^{uvi}] &= \frac{(1-v)n}{1-2v}D^{i00-1}_{ujv\bar{l}}H^{00}_{ukv\bar{m}} \frac{vn}{1-2v}D^{i100}_{ujv\bar{l}}H^{00}_{ukv\bar{m}} + \frac{n}{2}\left(D^{i00-1}_{ujv\bar{l}} - D^{i010}_{ujv\bar{l}}\right)H^{00}_{ukv\bar{m}}; \\
[K^{uwi}] &= \frac{v}{(1-2v)\gamma_i}\left(D^{i101}_{ujw\bar{p}} + D^{i000}_{ujw\bar{p}}\right)H^{01}_{ukw\bar{q}} + \frac{1}{2\gamma_i}D^{i011}_{ujw\bar{p}}H^{10}_{ukw\bar{q}}; \\
[K^{vvi}] &= \frac{(1-v)n^2}{1-2v}D^{i00-1}_{vlv\bar{l}}H^{00}_{vmv\bar{m}} + \frac{1}{2}\left(D^{i111}_{vlv\bar{l}} + D^{i00-1}_{vlv\bar{l}} - D^{i010}_{vlv\bar{l}} - D^{i100}_{vlv\bar{l}}\right)H^{00}_{vmv\bar{m}} + \frac{1}{2\gamma_i^2}D^{i001}_{vlv\bar{l}}H^{11}_{vmv\bar{m}}; \\
[K^{vwi}] &= \frac{vn}{(1-2v)\gamma_i}D^{i000}_{vlw\bar{p}}H^{01}_{vmw\bar{q}} + \frac{n}{2\gamma_i}D^{i000}_{vlw\bar{p}}H^{10}_{vmw\bar{q}}; \\
[K^{wwi}] &= \frac{1-v}{(1-2v)\gamma_i^2}D^{i001}_{wpw\bar{p}}H^{11}_{wqw\bar{q}} + \frac{1}{2}\left(D^{i111}_{wpw\bar{p}} + n^2 D^{i00-1}_{wpw\bar{p}}\right)H^{00}_{wqw\bar{q}}; \\
[M^{uui}] &= D^{i001}_{j\bar{j}}H^{00}_{uku\bar{k}}/8; \quad [M^{vvi}] = D^{i001}_{vlv\bar{l}}H^{00}_{vmv\bar{m}}/8; \\
[M^{wwi}] &= D^{i001}_{wpw\bar{p}}H^{00}_{wqw\bar{q}}/8
\end{aligned}
\tag{21}
$$

in which

$$
\begin{aligned}
D^{iabc}_{\alpha\sigma\beta\tau} &= \int_{-1}^{1}\frac{\mathrm{d}^a[\Phi^i_{\alpha}(\bar{r}_i)F_{\sigma}(\bar{r}_i)]}{\mathrm{d}\bar{r}_i^a}\frac{\mathrm{d}^b[\Phi^i_{\beta}(\bar{r}_i)F_{\tau}(\bar{r}_i)]}{\mathrm{d}\bar{r}_i^b}(\bar{r}_i+\delta_i)^c\,\mathrm{d}\bar{r}_i; \\
H^{ab}_{\alpha\sigma\beta\tau} &= \int_{-1}^{1}\frac{\mathrm{d}^a[\Psi^i_{\alpha}(\bar{z})F_{\sigma}(\bar{z})]}{\mathrm{d}\bar{z}^a}\frac{\mathrm{d}^b[\Psi^i_{\beta}(\bar{z})F_{\tau}(\bar{z})]}{\mathrm{d}\bar{z}^b}\,\mathrm{d}\bar{z}, \quad a,b=0,1;\ \ c=0,1,-1; \\
&\alpha,\beta=u,v,w; \quad \sigma=j,l,p,k,m,q; \quad \tau=\bar{j},\bar{l},\bar{p},\bar{k},\bar{m},\bar{q}.
\end{aligned}
\tag{22}
$$

Eq. (16) can be further expressed simply to

$$
([K]-\Omega^2[M])\{X\}=\{0\}, \tag{23}
$$

where

$$
[K]=\begin{bmatrix}[K^1] & [0]\\ [0] & [K^2]\end{bmatrix}; \quad [M]=\begin{bmatrix}[M^1] & [0]\\ [0] & [M^2]\end{bmatrix}; \quad \{X\}=\begin{Bmatrix}\{X^1\}\\ \{X^2\}\end{Bmatrix}. \tag{24}
$$

It should be mentioned that the two sets ($i=1,2$) in Eq. (16) are independent of each other, and therefore the eigenfrequencies of the plate could not be obtained directly from Eq. (23). This is because the column vector $\{X\}$ is not composed of independent variables which should also satisfy the displacement continuity conditions on the adjacent boundary of two sub-plates as follows

$$
\begin{aligned}
&\overline{U}_1(\bar{r}_1,\bar{z})=\overline{U}_2(\bar{r}_2,\bar{z}); \quad \overline{V}_1(\bar{r}_1,\bar{z})=\overline{V}_2(\bar{r}_2,\bar{z}); \\
&\overline{W}_1(\bar{r}_1,\bar{z})=\overline{W}_2(\bar{r}_2,\bar{z}), \quad \text{at } \bar{r}_1=1 \quad \text{and } \bar{r}_2=-1.
\end{aligned}
\tag{25}
$$

Substituting Eq. (10) into the above equation, one has

$$\begin{aligned}
&\sum_{j=1}^{J_i}\sum_{k=1}^{K_i} A^i_{jk}F_j(1)F_k(\bar{z}) = \Phi^2_u(-1)\Psi^2_u(\bar{z})\sum_{j=1}^{J_{i+1}}\sum_{k=1}^{K_{i+1}} A^{i+1}_{jk}F_j(-1)F_k(\bar{z});\\
&\sum_{l=1}^{L_i}\sum_{m=1}^{M_i} B^i_{lm}F_l(1)F_m(\bar{z}) = \Phi^2_v(-1)\Psi^2_v(\bar{z})\sum_{l=1}^{L_{i+1}}\sum_{m=1}^{M_{i+1}} B^{i+1}_{lm}F_l(-1)F_m(\bar{z});\\
&\sum_{p=1}^{P_i}\sum_{q=1}^{Q_i} C^i_{pq}F_p(1)F_q(\bar{z}) = \Phi^2_w(-1)\Psi^2_w(\bar{z})\sum_{p=1}^{P_{i+1}}\sum_{q=1}^{Q_{i+1}} C^{i+1}_{pq}F_p(-1)F_q(\bar{z}).
\end{aligned} \tag{26}$$

One may consider the following mathematical properties of Chebyshev polynomial series

$$\begin{aligned}
&F_s(1) = 1; \quad F_s(-1) = (-1)^{s-1};\\
&\int_{-1}^{1} F_s(\bar{z})F_t(\bar{z})/\sqrt{1-\bar{z}^2}\,\mathrm{d}\bar{z} = \begin{cases} 0 & s \neq t,\\ 1 & s = t \end{cases}
\end{aligned} \tag{27}$$

and then expand the two sides of Eq. (26) into a Chebyshev polynomial series in terms of the variable $\bar{z}$. For a solid circular plate one has

$$\begin{aligned}
&\sum_{j=1}^{J_1} A^1_{jk} = \Phi^2_u(-1)\sum_{j=1}^{J_2}\sum_{\bar{k}=1}^{K_2} A^2_{j\bar{k}}(-1)^{j-1}G_{k\bar{k}}, \quad k = 1,2,\ldots,K_1;\\
&\sum_{l=1}^{L_1} B^1_{lm} = \Phi^2_v(-1)\sum_{l=1}^{L_2}\sum_{\bar{m}=1}^{M_2} B^2_{l\bar{m}}(-1)^{l-1}G_{m\bar{m}}, \quad m = 1,2,\ldots,M_1;\\
&\sum_{p=1}^{P_1} C^1_{pq} = \Phi^2_w(-1)\sum_{p=1}^{P_2}\sum_{\bar{q}=1}^{Q_2} C^2_{p\bar{q}}(-1)^{p-1}G_{q\bar{q}}, \quad q = 1,2,\ldots,Q_1,
\end{aligned} \tag{28}$$

where

$$G_{st} = \int_{-1}^{1}\sqrt{1-\bar{z}^2}F_s(\bar{z})F_t(\bar{z})\,\mathrm{d}\bar{z}, \quad s = k,m,q; \;\; t = \bar{k},\bar{m},\bar{q}. \tag{29}$$

From Eq. (28), one knows that the number of independent unknowns is $N = \sum_{i=1}^{2}(J_i \times K_i + L_i \times M_i + P_i \times Q_i) - (K_1 + M_1 + Q_1)$. Selecting N variables in $\{X\}$ to make up a new column vector $\{\overline{X}\}$, then one has

$$\{X\} = [S]\{\overline{X}\}, \tag{30}$$

where the coefficient matrix $[S]$ is determined by Eq. (28). Using the above equation, Eq. (23) can be written as

$$([\overline{K}] - \Omega^2[\overline{M}])\{\overline{X}\} = \{0\} \tag{31}$$

where

$$[\overline{K}] = [S]^{\mathrm{T}}[K][S]; \quad [\overline{M}] = [S]^{\mathrm{T}}[M][S]. \tag{32}$$

A non-trivial solution is obtained by setting the determinant of the coefficient matrix of Eq. (31) equal to zero. The roots of the determinant are the square of the eigenvalue (dimensionless eigenfrequency) Ω. The eigenfunctions (mode shapes) corresponding to the eigenvalues are determined by back-substitution of the eigenvalues, one by one, in the usual manner.

3. Convergence and comparison studies

It is well known that the Ritz method provides eigenvalues converging as upper bounds to the exact values. Although solutions with any accuracy can be obtained theoretically by using a sufficiently large number of terms of admissible functions, a limit to the number of terms of admissible functions exists in the actual computation because of the limited speed, capacity and numerical accuracy of computers. Especially for the 3-D vibration analysis of structures, an ill-conditioned eigenvalue problem sometimes occurs due to the large matrix size involved. Therefore, it is important to study the convergence rate and the accuracy of the method. Firstly, a fully built-in, solid circular plate with the size parameters $h/R_1 = 0.5$ and $R_2/R_1 = 1.5$ is taken to show the convergence of the present method. In all the following computations, the Poisson's ratio $v = 0.3$ is used. For simplicity, equal numbers of terms of Chebyshev polynomials were taken for each of the displacement amplitude functions $\overline{U}$, $\overline{V}$ and $\overline{W}$ in each coordinate direction (namely $J_1 = L_1 = P_1 = J_2 = L_2 = P_2 = J$ and $K_1 = M_1 = Q_1 = K_2 = M_2 = Q_2 = K$), although using unequal numbers of series terms may be more efficient. Tables 1 and 2 give the convergence of the first eight eigenfrequency parameters for antisymmetric and symmetric modes, respectively, where only the torsional vibration, axisymmetric vibration and vibrations of circumferential wave numbers $n = 1$ and $n = 10$ were considered. Four groups of different numbers of terms were used to examine the convergence: $J \times K = 10 \times 5$, 15×10, 20×10 and 25×20. From the tables, one can see that with the increase of the numbers of terms, the eigenfrequency parameters monotonically decrease and the convergence patterns are similar for all of the mode categories. It is shown that the maximum relative error estimated from results by $J \times K = 20 \times 10$ and 25×20 is only about 0.065%, which occurs with the first antisymmetric mode of axisymmetric vibration. Such accuracy is more than sufficient for engineering applications. Moreover, with decreasing plate thickness, more terms in the radial direction but fewer terms in the thickness direction are needed.

The first eight eigenfrequency parameters of antisymmetric modes for the axisymmetric vibration and vibrations of circumferential wave numbers $n = 1, 2, 3$ are given in Table 3 and compared to those from classical plate theory (Leissa, 1969). The plate thickness ratio is $h/R_1 = 0.001$ and the built-in radius ratio

Table 1
Convergence of the first eight eigenfrequencies $\Omega = \omega R_1\sqrt{\rho/G}$ for the antisymmetric modes of a fully built-in solid circular plate, $R_2/R_1 = 1.5$; $h/R_1 = 0.5$

n	$J \times K$	Ω_1	Ω_2	Ω_3	Ω_4	Ω_5	Ω_6	Ω_7	Ω_8
0^t	10×5	7.253	9.118	11.37	13.36	14.34	16.16	17.74	19.19
	15×10	7.250	9.112	11.36	13.35	14.34	16.13	17.63	19.19
	20×10	7.250	9.109	11.36	13.35	14.34	16.13	17.63	19.19
	25×20	7.249	9.108	11.36	13.35	14.34	16.13	17.63	19.19
0^a	10×5	1.562	4.078	6.678	8.587	9.660	11.32	12.43	12.86
	15×10	1.557	4.068	6.666	8.577	9.643	11.31	12.41	12.86
	20×10	1.555	4.064	6.660	8.574	9.637	11.30	12.41	12.86
	25×20	1.554	4.063	6.658	8.572	9.634	11.30	12.41	12.86
1	10×5	2.651	5.297	7.008	8.011	8.150	9.947	10.19	11.10
	15×10	2.644	5.286	7.003	8.002	8.141	9.934	10.18	11.08
	20×10	2.641	5.281	7.002	7.998	8.137	9.930	10.18	11.07
	25×20	2.640	5.280	7.002	7.996	8.136	9.929	10.18	11.07
10	10×5	11.87	13.32	14.92	15.31	16.42	16.89	18.08	18.45
	15×10	11.86	13.32	14.90	15.30	16.42	16.86	18.07	18.44
	20×10	11.85	13.32	14.90	15.30	16.41	16.86	18.07	18.43
	25×20	11.85	13.32	14.90	15.30	16.41	16.86	18.07	18.43

Note: 0^t means torsional vibration, 0^a means axisymmetric vibration.

Table 2
Convergence of the first eight eigenfrequencies $\Omega = \omega R_1\sqrt{\rho/G}$ for the symmetric modes of a fully built-in solid circular plate, $R_2/R_1 = 1.5$; $h/R_1 = 0.5$

n	$J \times K$	Ω_1	Ω_2	Ω_3	Ω_4	Ω_5	Ω_6	Ω_7	Ω_8
0[t]	10×5	3.437	6.122	8.021	9.638	11.66	13.09	13.53	14.27
	15×10	3.433	6.115	8.020	9.635	11.66	13.08	13.53	14.27
	20×10	3.431	6.112	8.020	9.633	11.66	13.08	13.52	14.26
	25×20	3.430	6.111	8.020	9.633	11.66	13.08	13.52	14.26
0[a]	10×5	5.351	8.197	9.979	11.15	11.49	12.56	13.28	14.04
	15×10	5.343	8.194	9.973	11.15	11.48	12.54	13.27	14.02
	20×10	5.341	8.193	9.971	11.15	11.48	12.54	13.27	14.01
	25×20	5.340	8.192	9.670	11.15	11.48	12.54	13.27	14.01
1	10×5	2.878	4.781	6.871	7.286	8.729	9.126	10.64	10.75
	15×10	2.872	4.774	6.865	7.281	8.728	9.123	10.63	10.74
	20×10	2.871	4.772	6.863	7.279	8.728	9.121	10.63	10.74
	25×20	2.870	4.771	6.862	7.278	8.728	9.120	10.63	10.74
10	10×5	11.76	13.48	13.97	15.22	16.54	16.77	18.29	18.78
	15×10	11.76	13.47	13.95	15.22	16.53	16.75	18.26	18.75
	20×10	11.76	13.47	13.94	15.22	16.52	16.74	18.26	18.75
	25×20	11.76	13.47	13.94	15.22	16.52	16.74	18.26	18.75

Table 3
Comparison of the first eight eigenfrequency parameters λ of antisymmetric modes for a thin built-in solid circular plate ($h/R_1 = 0.001$, $R_2/R_1 = 1.25$) with the results from classical plate theory (in parentheses) by Leissa (1969)

n	λ_1	λ_2	λ_3	λ_4	λ_5	λ_6	λ_7	λ_8
0[a]	10.216	39.768	89.103	158.18	247.00	355.55	483.83	631.84
	(10.216)	(39.771)	(89.104)	(158.18)	(247.01)	(355.57)	(483.87)	(631.91)
1	21.259	60.828	120.08	199.05	297.74	416.17	554.33	712.21
	(21.26)	(60.82)	(120.08)	(199.06)	(297.77)	(416.20)	(554.37)	(712.30)
2	34.874	84.580	153.81	242.71	351.31	479.63	627.67	795.43
	(34.88)	(84.58)	(153.81)	(242.71)	(351.38)	(479.65)	(627.75)	(795.52)
3	51.031	111.02	190.30	289.17	407.70	545.93	703.86	881.51
	(51.04)	(111.01)	(190.30)	(289.17)	(407.72)	(545.97)	(703.95)	(881.67)

is $R_2/R_1 = 1.25$. In the computation, $30\times\ 2$ terms of the admissible functions were used and both built-in end conditions are considered. However, the results show that no difference between these two different built-in end conditions has been found for such a very thin plate. To facilitate comparison, the dimensionless eigenfrequency parameter $\lambda = \omega R_1^2\sqrt{\rho h/D}$ is used, where D is the flexural rigidity of the plate. Very good agreement is observed for all cases. It should be mentioned that the case of a very thin circular plate ($h/R_1 = 0.001$) is a stringent test case for 3-D vibration analysis. This again shows that the present method possesses rather good stability in numerical computation.

In order to further demonstrate the reliability and accuracy of the present method, a comparison with the finite element solutions for axisymmetric vibration of solid circular plates are given in Table 4 for the fully built-in condition and the built-in condition with a free edge. Three different plate thickness ratios $h/R_1 = 0.25$, 0.5 and 1.0, and two different built-in radius ratios $R_2/R_1 = 1.05$ and 1.25 are considered. In the finite element computation, shear modulus $G = 1.0$, mass density per unit volume $\rho = 1.0$ and free surface radius $R_1 = 1.0$ are taken. The QUAD8 axisymmetric element in the commercial program

Table 4
Comparison of the present solutions for axisymmetric vibration with finite element solutions shown in parentheses

R_1/R_2	h/R_1	Ω_1	Ω_2	Ω_3	Ω_4	Ω_5	Ω_6	Ω_7	Ω_8
Fully built-in solid circular plates									
1.05	0.25	1.049	3.296	6.002	6.267*	8.871	11.25*	11.79	14.16
		(1.060)	(3.321)	(6.026)	(6.286)	(8.875)	(11.26)	(11.75)	(14.10)
	0.5	1.602	4.185	6.131*	7.008	8.968	9.472*	10.07	10.91*
		(1.613)	(4.199)	(6.143)	(7.004)	(8.957)	(9.449)	(10.05)	(10.86)
	1.0	1.976	4.672	5.067*	6.339*	6.707	6.995*	7.637	8.095*
		(1.983)	(4.673)	(5.061)	(6.340)	(6.707)	(6.992)	(7.631)	(8.079)
1.25	0.25	1.036	3.273	5.967	5.980*	8.802	10.62*	11.65	14.01
		(1.051)	(3.305)	(5.998)	(6.025)	(8.812)	(10.67)	(11.62)	(13.97)
	0.5	1.558	4.068	5.615*	6.673	8.614	8.812*	9.677	10.34*
		(1.575)	(4.092)	(5.639)	(6.685)	(8.632)	(8.792)	(9.673)	(10.30)
	1.0	1.869	4.224	4.723*	6.045*	6.139	6.506*	7.080	7.766*
		(1.883)	(4.235)	(4.719)	(6.038)	(6.145)	(6.521)	(7.089)	(7.760)
Built-in solid circular plates with free end									
1.05	0.25	1.014	3.243	5.304*	5.926	8.715	9.559*	11.45	13.50*
		(1.033)	(3.280)	(5.407)	(5.966)	(8.747)	(9.640)	(11.47)	(13.49)
	0.5	1.484	3.865	4.203*	6.066	7.898*	8.022	9.394	10.09*
		(1.510)	(3.912)	(4.252)	(6.123)	(7.892)	(8.074)	(9.416)	(10.06)
	1.0	1.624	3.286*	3.319	5.140	5.474*	6.134*	6.559	7.111*
		(1.655)	(3.292)	(3.355)	(5.168)	(5.481)	(6.168)	(6.571)	(7.134)
1.25	0.25	1.035	3.273	5.903*	5.967	8.802	10.24*	11.65	13.09*
		(1.051)	(3.305)	(5.957)	(5.997)	(8.812)	(10.31)	(11.62)	(13.09)
	0.5	1.550	4.055	4.735*	6.640	7.439*	8.514	9.561	9.766*
		(1.568)	(4.081)	(4.777)	(6.655)	(7.445)	(8.542)	(9.564)	(9.733)
	1.0	1.808	3.192*	3.905	5.269	5.409*	6.166	6.326*	7.414
		(1.825)	(3.201)	(3.925)	(5.290)	(5.404)	(6.166)	(6.346)	(7.408)

Note: Values with asterisk are the symmetric modes in the thickness direction.

STRAND7 (G+D Computing Pty Ltd, 1999) is used to obtain the results. The inner sub-plate is divided into 20 elements in the radial direction while the outer sub-plate is divided into 4 elements in the radial direction. The size of each element in the thickness direction is fixed at $0.0625R_1$. It is shown that the present solutions are in very good agreement with the finite element solutions for all cases.

4. Parametric studies

This section describes in detail investigations in the effects of various parameters on the vibrational characteristics of built-in solid circular plates. They are the thickness ratio h/R_1 the built-in radius ratio R_2/R_1 and the end condition of the plate at $r = R_2$ Tables 5 and 6 give, respectively, the first eight eigenfrequency parameters for the antisymmetric and symmetric modes of a fully built-in circular plate with thickness ratio $h/R_1 = 0.5$. Six different built-in radius ratios, namely $R_2/R_1 = 1.01$, 1.05, 1.1, 1.5, 2.0 and 3.0 were considered. It is shown that the flexibility of the built-in part always results in decreasing eigenfrequencies. In most cases, the eigenfrequency parameters monotonically decrease with increasing built-in length, especially for built-in radius ratio $R_2/R_1 \leqslant 2$. The only exception is the second eigenfrequency parameters of the antisymmetric mode for torsional vibration for $R_2/R_1 = 3.0$ and 5.0. In these two cases, the eigenfrequency parameters are only slightly larger than the eigenfrequency parameter for $R_2/R_1 = 2.0$. Moreover, with an increase of the built-in radius ratio, the eigenfrequency parameters approach constant values sooner or later accord-

Table 5
The first eight eigenfrequencies $\Omega = \omega R_1\sqrt{\rho/G}$ for the antisymmetric modes of a fully built-in solid circular plate, $h/R_1 = 0.5$

n	R_2/R_1	Ω_1	Ω_2	Ω_3	Ω_4	Ω_5	Ω_6	Ω_7	Ω_8
0^t	1.01	7.341	9.370	11.88	14.62	17.49	19.23	20.09	20.42
	1.05	7.292	9.240	11.66	14.31	17.07	19.21	19.87	20.06
	1.1	7.265	9.164	11.52	14.08	16.71	19.13	19.35	20.03
	1.5	7.250	9.109	11.36	13.35	14.34	16.13	17.63	19.19
	2.0	7.250	9.109	11.36	12.89	13.53	14.24	15.40	16.55
	3.0	7.250	9.110	11.36	12.66	12.92	13.29	13.70	14.17
	5.0	7.250	9.110	11.36	12.59	12.67	12.78	12.94	13.13
0^a	1.01	1.642	4.304	7.249	9.092	10.37	12.81	13.45	16.07
	1.05	1.602	4.186	7.009	8.958	10.07	12.49	13.16	15.65
	1.1	1.579	4.115	6.827	8.818	9.863	12.14	12.99	15.18
	1.5	1.555	4.064	6.661	8.574	9.637	11.30	12.41	12.86
	2.0	1.555	4.064	6.660	8.573	9.629	11.13	11.55	11.92
	3.0	1.555	4.063	6.659	8.572	9.627	11.03	11.13	11.28
	5.0	1.555	4.063	6.659	8.572	9.627	10.99	11.00	11.07
1	1.01	2.776	5.671	7.171	8.240	8.759	10.48	10.89	11.88
	1.05	2.707	5.497	7.124	8.151	8.483	10.30	10.68	11.57
	1.1	2.670	5.376	7.077	8.091	8.284	10.19	10.47	11.37
	1.5	2.641	5.282	7.003	7.998	8.138	9.931	10.18	11.08
	2.0	2.641	5.282	7.003	7.997	8.137	9.922	10.18	11.02
	3.0	2.640	5.281	7.003	7.997	8.137	9.922	10.18	10.99
	5.0	2.640	5.280	7.003	7.996	8.136	9.922	10.18	10.98
2	1.01	3.918	6.989	8.219	9.305	10.19	11.63	12.53	13.31
	1.05	3.810	6.756	8.137	9.172	9.881	11.42	12.24	12.99
	1.1	3.745	6.579	8.066	9.077	9.658	11.28	11.93	12.80
	1.5	3.701	6.420	7.945	8.953	9.434	11.08	11.21	12.31
	2.0	3.701	6.419	7.945	8.952	9.429	10.99	11.15	11.49
	3.0	3.700	6.419	7.945	8.952	9.429	10.95	11.11	11.13
	5.0	3.700	6.419	7.945	8.952	9.429	10.94	11.00	11.03

ing to the order of eigenfrequencies. However the rate of eigenfrequencies of the antisymmetric mode in approaching constant values, with respect to the built-in length, is much more rapid than that of the symmetric mode. In general, for $R_2/R_1 > 1.5$, the effect of the built-in length on the first three eigenfrequency parameters of antisymmetric mode can be neglected.

The first eight eigenfrequency parameters for the antisymmetric and symmetric modes of the same plate with built-in condition but having a free end are, respectively, given in Tables 7 and 8. It is shown that for the antisymmetric modes, the first three eigenfrequency parameters for $n = 0^t$ (i.e. torsional vibration); the first five for $n = 0^a$ (i.e. axisymmetric vibration); the first seven for $n = 1$ and the first six for $n = 2$ monotonically increase with increasing built-in radius ratio. For the symmetric modes, the first two eigenfrequency parameters for $n = 0^t$; the first for $n = 0^a$; the first two for $n = 1$ and the first two for $n = 2$ also monotonically increase with increasing built-in radius ratio. Similar to the plate with fully built-in condition, with the increase of the built-in length, the eigenfrequency parameters also approach constant values sooner or later according to the order of eigenfrequencies. However, the rate of eigenfrequencies of the antisymmetric mode in approaching constant values, with respect to the built-in length, is much more rapid than that of the symmetric mode. In general, for $R_2/R_1 > 1.5$, the effect of the built-in length on at least the first three eigenfrequency parameters of antisymmetric mode can be neglected.

Table 6
The first eight eigenfrequencies $\Omega = \omega R_1\sqrt{\rho/G}$ for the symmetric modes of a fully built-in solid circular plate, $h/R_1 = 0.5$

n	R_2/R_1	Ω_1	Ω_2	Ω_3	Ω_4	Ω_5	Ω_6	Ω_7	Ω_8
0^t	1.01	3.795	6.948	10.07	13.13	13.19	14.36	16.11	16.31
	1.05	3.677	6.730	9.756	12.76	13.10	14.27	15.74	15.98
	1.1	3.578	6.541	9.457	12.32	13.09	14.20	15.14	15.91
	1.5	3.431	6.113	8.020	9.634	11.66	13.08	13.52	14.27
	2.0	3.429	6.058	7.038	8.281	9.434	10.83	12.27	13.08
	3.0	3.428	6.049	6.514	7.036	7.737	8.498	9.248	10.08
	5.0	3.428	6.048	6.344	6.497	6.731	7.032	7.390	7.791
0^a	1.01	6.290	9.608	11.01	11.41	12.61	13.43	14.46	15.41
	1.05	6.132	9.473	10.90	11.32	12.51	13.12	14.21	15.24
	1.1	5.965	9.312	10.75	11.26	12.41	12.85	14.07	15.05
	1.5	5.341	8.193	9.971	11.15	11.48	12.54	13.27	14.01
	2.0	5.221	7.527	9.129	10.22	11.18	11.61	12.54	13.13
	3.0	5.206	6.844	7.776	8.889	9.906	10.76	11.20	11.78
	5.0	5.206	6.457	6.860	7.398	7.996	8.688	9.436	10.02
1	1.01	3.303	5.317	8.171	8.542	10.42	11.45	11.58	11.87
	1.05	3.212	5.151	7.973	8.310	10.27	11.21	11.43	11.67
	1.1	3.124	5.012	7.763	8.101	10.08	10.86	11.37	11.50
	1.5	2.871	4.772	6.863	7.279	8.728	9.121	10.63	10.74
	2.0	2.847	4.763	6.552	6.852	7.565	8.371	8.800	9.667
	3.0	2.847	4.763	6.408	6.507	6.863	7.244	7.378	8.009
	5.0	2.847	4.762	6.336	6.365	6.480	6.606	6.681	6.939
2	1.01	5.125	6.808	9.338	9.940	11.02	12.18	12.83	13.29
	1.05	4.988	6.603	9.157	9.677	10.87	12.09	12.46	12.93
	1.1	4.852	6.425	8.936	9.453	10.69	12.02	12.12	12.57
	1.5	4.406	6.052	7.810	8.307	9.564	9.910	11.28	11.64
	2.0	4.350	5.998	7.248	7.404	8.240	9.153	9.442	10.22
	3.0	4.347	5.982	6.661	6.819	7.231	7.697	7.832	8.483
	5.0	4.347	5.980	6.396	6.458	6.665	6.741	6.957	7.111

Comparing the results in Tables 5 and 6 with those in Tables 7 and 8, one can see that the eigenfrequencies of a plate with fully built-in condition are always higher than those with built-in condition but having a free end. With the increase of the built-in radius ratio, the eigenfrequencies of a plate with fully built-in condition gradually coincide with those of the plate with built-in condition but having a free end. In general for $R_2/R_1 \geqslant 2$, the effect of the end condition on eigenfrequencies can be ignored, especially for the antisymmetric mode. This means that for a plate with sufficient built-in length, its end condition is immaterial. Moreover, the effect of the built-in length on symmetric modes is more significant than that on antisymmetric modes for both built-in end conditions.

The effect of the thickness ratio on the first two eigenfrequency parameters of various mode categories for the built-in solid circular plates with free end was studied and presented in Figs. 2–7. The plates have a fixed built-in radius ratio $R_2/R_1 = 1.25$. The error function $e = (\omega_c - \omega)/\omega$ is defined to evaluate the differences between the present solutions (eigenfrequency ω) considering the flexibility of the built-in part and the 3-D solutions (eigenfrequencies ω_c) ignoring the flexibility of the built-in part, which is referred to as the classical clamped boundary condition. In particular, the classical clamped boundary condition is equivalent to having a clamped end at R_1 Six different vibration categories were considered: $n = 0^t$; $n = 0^a$ and $n = 1$–4. The thickness ratio varies from 0 to 1 with an increment of 0.1. It is seen that in most cases, the errors monotonically increase with increase in plate thickness, except for the first symmetric mode of axisymmetric

Table 7
The first eight eigenfrequencies $\Omega = \omega R_1\sqrt{\rho/G}$ for the antisymmetric modes of a built-in solid circular plate with free end, $h/R_1 = 0.5$

n	R_2/R_1	Ω_1	Ω_2	Ω_3	Ω_4	Ω_5	Ω_6	Ω_7	Ω_8
0[t]	1.01	7.023	8.663	10.90	13.46	16.18	18.85	19.23	19.88
	1.05	7.181	8.921	11.07	13.41	15.85	18.35	19.22	20.00
	1.1	7.228	9.034	11.18	13.30	15.38	17.73	19.21	20.02
	1.5	7.250	9.109	11.36	12.71	13.72	15.16	16.81	18.54
	2.0	7.250	9.109	11.36	12.60	13.17	13.81	14.75	15.98
	3.0	7.250	9.110	11.36	12.57	12.76	13.08	13.48	13.90
	5.0	7.250	9.110	11.36	12.57	12.62	12.71	12.85	13.02
0[a]	1.01	1.388	3.383	5.469	7.809	9.268	11.00	12.34	14.33
	1.05	1.485	3.868	6.071	8.026	9.397	10.97	12.33	14.05
	1.1	1.521	4.002	6.427	8.219	9.471	10.96	12.18	13.78
	1.5	1.555	4.063	6.658	8.570	9.613	10.87	11.47	11.76
	2.0	1.555	4.063	6.659	8.572	9.627	10.85	11.00	11.42
	3.0	1.555	4.063	6.659	8.572	9.627	10.84	10.97	11.11
	5.0	1.555	4.063	6.659	8.572	9.627	10.84	10.97	11.00
1	1.01	2.333	4.217	6.430	7.445	7.719	9.212	9.724	10.80
	1.05	2.549	4.893	6.689	7.635	7.973	9.374	9.938	10.89
	1.1	2.606	5.155	6.855	7.807	8.065	9.508	10.05	10.89
	1.5	2.641	5.279	7.002	7.995	8.135	9.905	10.17	10.90
	2.0	2.641	5.280	7.003	7.995	8.136	9.921	10.18	10.82
	3.0	2.640	5.280	7.003	7.996	8.136	9.923	10.18	10.84
	5.0	2.640	5.280	7.003	7.996	8.136	9.923	10.18	10.86
2	1.01	3.100	5.207	7.404	8.512	8.887	10.38	10.98	12.20
	1.05	3.527	5.841	7.602	8.696	9.151	10.57	11.04	12.19
	1.1	3.645	6.193	7.738	8.796	9.278	10.68	11.07	12.09
	1.5	3.700	6.418	7.944	8.949	9.419	10.78	11.13	11.49
	2.0	3.700	6.419	7.945	8.952	9.429	10.81	10.95	11.14
	3.0	3.700	6.419	7.945	8.952	9.429	10.83	10.93	11.04
	5.0	3.700	6.419	7.945	8.952	9.429	10.94	11.00	11.03

vibration as shown in Fig. 3. Moreover, the effect of plate thickness on eigenfrequencies of symmetric modes is in general higher than that on the antisymmetric modes of the same order, especially for the thicker plates.

As no dimensional simplication has been made in the analysis, the results of the plate problems obtained by the use of the 3-D theory of elasticity are taken as reference solutions for results obtained by various approximate plate theories. Table 9 gives a comparison of the present solutions with those (Liew et al., 1997) from the Mindlin theory, which is commonly used for moderately thick plates. Five different thickness ratios (h/R_1 varying from 0.05 to 0.25 with an increment of 0.05) and the first six eigenfrequencies of axisymmetric vibration have been considered. It is shown from the table that the Mindlin theory can only predict the antisymmetric modes in the thickness direction, but it cannot predict the symmetric ones. In the range of plate thickness studied here, the eigenfrequencies from the Mindlin theory are always lower than those from 3-D elasticity theory for the classical boundary conditions. However, they are larger than those from 3-D elasticity theory for built-in boundary conditions, either with clamped end or free end. For thin plates such as $h/R_1 = 0.05$, the differences between the solutions of Mindlin theory and 3-D elasticity are very small. For thick plates such as $h/R_1 = 0.25$, the errors increase significantly especially when compared to the 3-D solutions which include the effect of the built-in part.

Table 8
The first eight eigenfrequencies $\Omega = \omega R_1\sqrt{\rho/G}$ for the symmetric modes of a built-in solid circular plate with free end, $h/R_1 = 0.5$

n	R_2/R_1	Ω_1	Ω_2	Ω_3	Ω_4	Ω_5	Ω_6	Ω_7	Ω_8
0[t]	1.01	2.448	5.478	8.550	11.60	12.98	13.90	14.75	15.52
	1.05	2.928	5.600	8.388	11.21	13.06	13.89	14.41	15.73
	1.1	3.162	5.680	8.154	10.75	13.08	13.48	14.28	15.82
	1.5	3.426	5.954	6.812	8.768	10.55	12.54	13.09	14.14
	2.0	3.428	6.032	6.412	7.579	8.817	10.05	11.54	12.93
	3.0	3.428	6.048	6.301	6.711	7.342	8.094	8.852	9.631
	5.0	3.428	6.048	6.285	6.398	6.593	6.863	7.195	7.577
0[a]	1.01	3.997	8.067	10.14	10.83	11.62	12.40	12.97	14.53
	1.05	4.206	7.898	10.09	11.11	11.77	12.50	13.50	14.37
	1.1	4.370	7.738	9.997	11.15	11.70	12.54	13.84	14.14
	1.5	5.030	7.077	9.225	10.46	11.21	12.00	12.62	14.01
	2.0	5.180	6.595	8.148	9.763	10.82	11.22	12.07	12.62
	3.0	5.203	6.314	7.226	8.228	9.435	10.22	11.14	11.35
	5.0	5.206	6.241	6.581	7.073	7.650	8.290	9.029	9.733
1	1.01	1.797	3.764	5.975	7.015	9.213	10.04	10.67	11.28
	1.05	2.144	4.169	5.954	6.993	9.084	9.785	10.88	11.34
	1.1	2.358	4.399	5.937	6.926	8.950	9.437	10.82	11.37
	1.5	2.812	4.747	6.133	6.525	7.656	8.222	9.619	9.936
	2.0	2.845	4.761	6.201	6.383	7.025	7.347	8.065	8.955
	3.0	2.847	4.762	6.221	6.332	6.561	6.709	7.086	7.628
	5.0	2.847	4.762	6.227	6.304	6.382	6.412	6.561	6.768
2	1.01	3.122	5.095	7.384	8.507	10.00	11.12	11.69	11.79
	1.05	3.410	5.430	7.265	8.387	9.928	11.08	11.62	12.00
	1.1	3.619	5.614	7.160	8.197	9.823	10.67	11.51	12.04
	1.5	4.259	5.896	6.916	7.001	8.574	9.244	10.27	10.73
	2.0	4.341	5.945	6.477	6.717	7.630	8.177	8.767	9.692
	3.0	4.347	5.977	6.267	6.474	6.933	7.121	7.476	8.090
	5.0	4.347	5.980	6.228	6.347	6.494	6.545	6.783	6.905

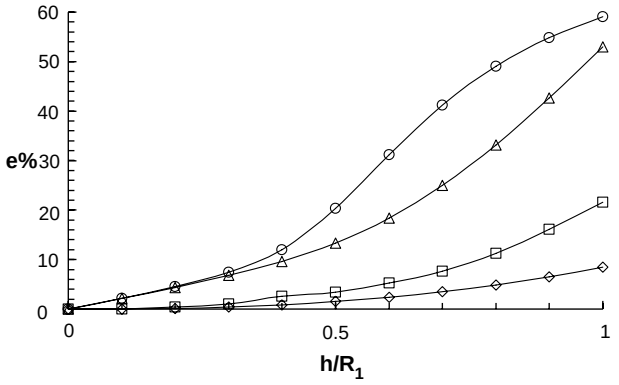

Fig. 2. The eigenfrequency errors of torsional vibration for solid circular plates, considering the flexibility of the built-in annulus via the classical boundary condition, $R_2/R_1 = 1.25$: (◇) the first antisymmetric mode; (□) the second antisymmetric mode; (△) the first symmetric mode; (○) the second symmetric mode.

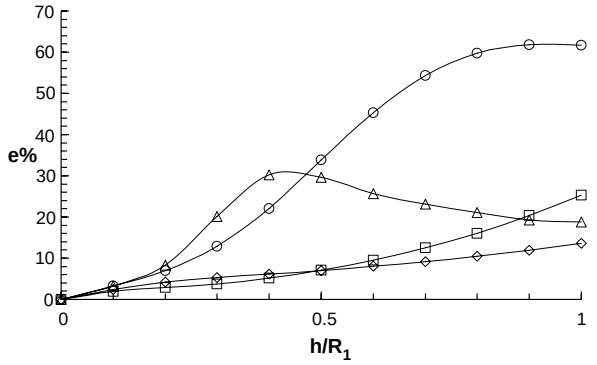

Fig. 3. The eigenfrequency errors of axisymmetric vibration for solid circular plates, considering the flexibility of the built-in annulus via the classical boundary condition, $R_2/R_1 = 1.25$: (◇) the first antisymmetric mode; (□) the second antisymmetric mode; (△) the first symmetric mode; (○) the second symmetric mode.

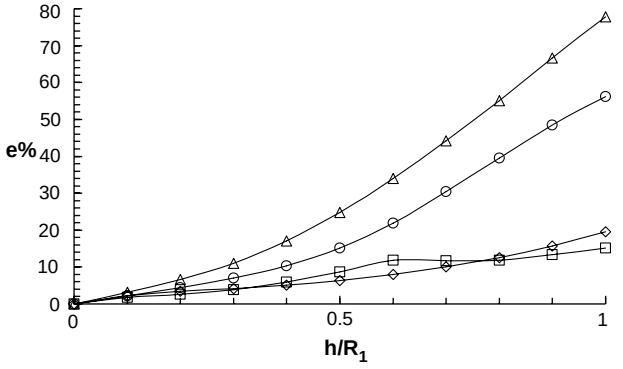

Fig. 4. The eigenfrequency errors of circumferential wave number $n = 1$ for solid circular plates, considering the flexibility of the built-in annulus via the classical boundary condition, $R_2/R_1 = 1.25$: (◇) the first antisymmetric mode; (□) the second antisymmetric mode; (△) the first symmetric mode; (○) the second symmetric mode.

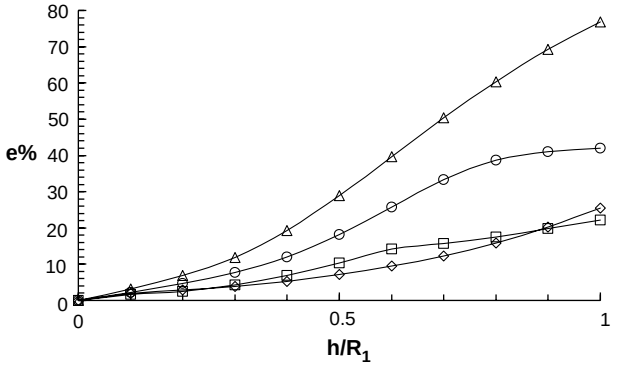

Fig. 5. The eigenfrequency errors of circumferential wave number $n = 2$ for solid circular plates, considering the flexibility of the built-in annulus via the classical boundary condition, $R_2/R_1 = 1.25$: (◇) the first antisymmetric mode; (□) the second antisymmetric mode; (△) the first symmetric mode; (○) the second symmetric mode.

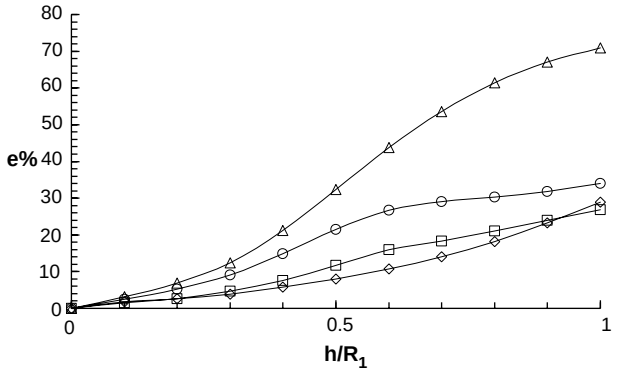

Fig. 6. The eigenfrequency errors of circumferential wave number $n = 3$ for solid circular plates, considering the flexibility of the built-in annulus via the classical boundary condition, $R_2/R_1 = 1.25$: (◇) the first antisymmetric mode; (□) the second antisymmetric mode; (△) the first symmetric mode; (○) the second symmetric mode.

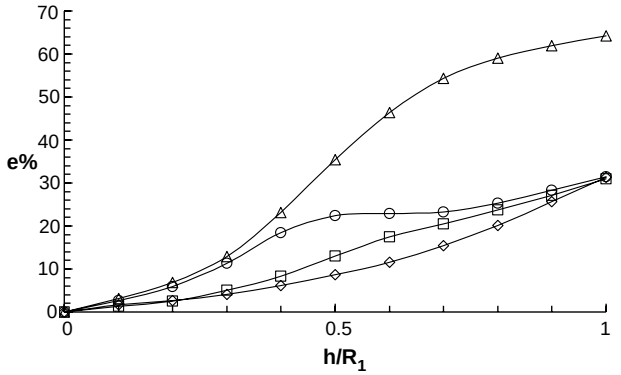

Fig. 7. The eigenfrequency errors of circumferential wave number $n = 4$ for solid circular plates, considering the flexibility of the built-in annulus via the classical boundary condition, $R_2/R_1 = 1.25$: (◇) the first antisymmetric mode; (□) the second antisymmetric mode; (△) the first symmetric mode; (○) the second symmetric mode.

5. Conclusions

The 3-D free vibration of circular plates, which are built into a rigid medium, is studied. The analysis is based on the theory of small-strain elasticity for isotropic materials. The eigenvalue equations are derived by the Ritz method. Using the Chebyshev polynomial series as the admissible functions, high accuracy and stable computations have been achieved as observed from the convergence and comparison studies. The effect of plate thickness, built-in length and the end condition on eigenfrequencies is investigated in detail. The following conclusions can be drawn:

1. The effect of the built-in part on eigenfrequencies significantly increases with increasing plate thickness. The effect of flexibility of the built-in part on the symmetric modes is higher than that on antisymmetric modes. For thin plates, the effect of the built-in part on eigenfrequencies is very small and can be ignored. However, for thick plates, the effect of the built-in part on eigenfrequencies is considerable and should be considered in the analysis.

Table 9
A comparison study of the present solutions with those from Mindlin theory for the axisymmetric vibration of solid built-in circular plates with $R_2/R_1 = 1.1$

h/R_1	Solution	λ_1	λ_2	λ_3	λ_4	λ_5	λ_6
0.05	3-D^{bc}	10.026	38.476	84.355	145.64	220.12	261.57
	3-D^{bf}	10.026	38.476	84.355	145.64	220.12	261.56
	3-D^{c}	10.159	38.938	85.263	147.05	222.02	265.72^{s}
	Mindlin	10.145	38.855	84.995	146.40	220.73	–
0.1	3-D^{bc}	9.7320	35.968	75.090	123.02	128.94	176.66
	3-D^{bf}	9.7319	35.967	75.088	123.02	128.47	176.66
	3-D^{c}	9.9728	36.682	76.305	124.73	132.91^{s}	178.94
	Mindlin	9.9408	36.479	75.664	123.32	–	176.41
0.15	3-D^{bc}	9.3662	32.911	65.172	85.050	101.97	141.04
	3-D^{bf}	9.3604	32.894	65.144	83.468	101.94	141.00
	3-D^{c}	9.6802	33.712	66.461	88.590^{s}	103.90	143.91
	Mindlin	9.6286	33.393	65.551	–	102.09	140.93
0.2	3-D^{bc}	8.9535	29.802	56.365	63.284	85.242	114.98
	3-D^{bf}	8.9247	29.737	56.279	60.353	85.140	114.85
	3-D^{c}	9.3111	30.616	57.736	66.392^{s}	87.526	118.59
	Mindlin	9.2400	30.211	56.682	–	85.571	115.55
0.25	3-D^{bc}	8.5220	26.899	49.001	50.318	72.287	80.272
	3-D^{bf}	8.4537	26.778	48.856	46.123	72.075	90.204
	3-D^{c}	8.8957	27.715	50.534	53.040^{s}	75.017	95.001^{s}
	Mindlin	8.8068	27.253	49.420	–	73.054	–

Note: 3-D^{c} means 3-D solutions of circular plates with classical clamped boundary. 3-D^{bc} means 3-D solutions of fully built-in circular plates and 3-D^{bf} means 3-D solutions of built-in circular plates with free end. The superscript s means symmetric modes in the thickness direction. The solutions of Mindlin theory are taken from a paper published by Liew et al. (1997).

2. For a circular plate with fully built-in edges, the flexibility of the built-in part always results in a decrease of eigenfrequencies. The eigenfrequencies of plates with fully built-in conditions are always higher than those of built-in plates with free end. For a plate with bigger built-in length or smaller thickness, the effect of the end condition on eigenfrequencies can be neglected, whether for plates with fully built-in condition or for plates with built-in condition but having a free end.
3. With the increase of the built-in length, the eigenfrequencies approach constant values sooner or later according to the order of eigenfrequencies. However, the rate of eigenfrequencies of the antisymmetric modes in approaching constant values, with respect to the built-in length, is much more rapid than that of the symmetric modes.

Acknowledgment

The work described in this paper was partially supported by a grant from the Research Grants Council of the Hong Kong Special Administrative Region, China (Project No: HKU7011/01E).

References

Deresiewicz, H., Mindlin, R.D., 1955. Axially symmetric flexural vibrations of a circular disk. ASME Journal of Applied Mechanics 49, 633–638.

Fan, J.R., Ye, J.Q., 1990. Exact solution for axisymmetric vibration of laminated circular plates. ASCE Journal of Engineering Mechanics 116, 20–27.

Fox, L., Parker, I.B., 1968. Chebyshev Polynomials in Numerical Analysis. Oxford University Press, London.

G+D Computing Pty Ltd, 1999. Using STRAND7, first ed. Sydney.

Hanna, N.F., Leissa, A.W., 1994. A higher order shear deformation theory for the vibration of thick plates. Journal of Sound and Vibration 170, 545–555.

Hutchinson, J.R., 1979. Axisymmetric flexural vibrations of a thick free circular plate. ASME Journal of Applied Mechanics 46, 139–144.

Hutchinson, J.R., 1984. Vibration of thick free circular plates, exact versus approximate solutions. ASME Journal of Applied Mechanics 51, 581–585.

Leissa, A.W., 1969. Vibration of Plates, NASA SP-160. Office of Technology Utilization, Washington, DC.

Liew, K.M., Yang, B., 1999. Three-dimensional elasticity solutions for free vibrations of circular plates: a polynomials-Ritz analysis. Computer Methods in Applied Mechanics and Engineering 175, 189–201.

Liew, K.M., Yang, B., 2000. Elasticity solutions for free vibrations of annular plates from three-dimensional analysis. International Journal of Solids and Structures 37, 7689–7702.

Liew, K.M., Han, J.-B., Xiao, Z.M., 1997. Vibration analysis of circular Mindlin plates using the differential quadrature method. Journal of Sound and Vibration 205, 617–630.

Liu, C.F., Lee, Y.T., 2000. Finite element analysis of three-dimensional vibrations of thick circular and annular plates. Journal of Sound and Vibration 233, 63–80.

Reddy, J.N., 1984. A simple higher-order theory for laminated composite plates. ASME Journal of Applied Mechanics 51, 745–752.

So, J., Leissa, A.W., 1998. Three-dimensional vibrations of thick circular and annular plates. Journal of Sound and Vibration 209, 15–41.

Zhou, D., Au, F.T.K., Cheung, Y.K., Lo, S.H., 2003a. Three-dimensional vibration analysis of circular and annular plates via the Chebyshev–Ritz method. International Journal of Solids and Structures 40, 3089–3105.

Zhou, D., Cheung, Y.K., Lo, S.H., Au, F.T.K., 2003b. 3D vibration analysis of solid and hollow circular cylinders via Chebyshev–Ritz method. Computer Methods in Applied Mechanics and Engineering 192, 1575–1589.